Impact Improvement Mechanism of HIPS with Bimodal Distribution of Rubber Particle Size†

Y. Okamoto,* H. Miyagi, and M. Kakugo

Chiba Research Laboratory, Sumitomo Chemical Company, Ltd., 2-1 Kitasode, Sodegaura, Chiba 299-02, Japan

K. Takahashi

Research Institute for Applied Mechanics, Kyushu University, 6-1 Kasugakoen, Kasuga, Fukuoka 816, Japan

Received November 1, 1990; Revised Manuscript Received May 7, 1991

ABSTRACT: The impact toughening mechanism of high-impact polystyrene (HIPS) with a bimodal distribution of rubber particle size (bimodal HIPS) was investigated through craze observation in a transmission electron microscope (TEM) and by nonlinear stress analysis around rubber particles by the finite element method (FEM). TEM observation revealed that (1) crazes are generated from large particles perpendicular to the tensile direction, (2) crazes grow in the direction of neighboring small rubber particles like bridges, and (3) the craze length of bimodal HIPS is longer than that of monomodal HIPS. FEM analysis indicated that stress is highly concentrated at the surface of a small rubber particle adjoining a large rubber particle. This stress concentration is greatly affected by the stress field of the large particle. Thus, in bimodal HIPS, (1) crazes are induced from the large particle's surface at the initial stage of loading, (2) as these crazes grow, minute crazes from small rubber particles in the vicinity of the large particle are induced, and then (3) they overlap with the crazes growing from the large particle and consequently, (4) long extended crazes from the surface of the large particle are formed under the stress field of bimodal rubber particles.

I. Introduction

It is well-known that the toughness of glassy polymers can be improved by the dispersion of rubber particles,[1,2] and the toughening mechanism of these systems has been studied extensively.[3-6] In high-impact polystyrene (HIPS), the absorption of impact energy is thought to increase mainly by the generation and growth of crazes in the polystyrene (PS) matrix.[7] Effects of the rubber content and rubber particle size on the toughening of HIPS have been studied from both scientific and technical aspects. In monomodal rubber particle HIPS (monomodal HIPS), the optimum rubber particle diameter known is 1–2 μm.[8,9] From a practical point of view, HIPS with a dual population of rubber particle sizes (bimodal HIPS) has been studied for its unique impact properties.[10,11] It has been shown that better impact toughness can be achieved in an optimum bimodal HIPS than in a monomodal one with the same rubber content.[12] However, few studies have been concerned with the cause of the increase in impact strength of bimodal HIPS. A model was recently presented to explain the craze growth mechanism in bimodal HIPS by using the finite element method (FEM).[13] This model assumed that small particles initiated crazes which propagated in the direction of large particles, where they were stopped.

In this work, the crazing process in bimodal HIPS was studied by observation with a transmission electron microscope (TEM). Nonlinear stress analysis around rubber particles was also performed by using FEM.

II. Experimental Section

Bimodal HIPS specimens were obtained by injection molding the blend of two monomodal HIPS, which had rubber particles of different average diameters. Characteristic data of the monomodal HIPS used in this study are summarized in Table I. Rubber particle sizes were estimated through TEM observation,

† Presented at the "Benibana" International Symposium, Yamagata, Japan, Oct 8–11, 1990.

Table I
Summary of Material Characteristics of Monomodal HIPS Used in Figure 3

sample	content, wt % rubber	content, wt % gel	ave rubber particle diameter D, μm	Izod impact strength, kg·cm/cm²
A	8.6	23.0	0.2	6.9
B	6.5	18.3	1.0	7.7
C	8.4	23.2	4.9	7.8

and rubber content was determined by iodine titration. Gel content was determined from the extract after the process of centrifuging the dissolved samples with mixture solvents (methyl ethyl ketone/methanol = 10/1 in volume ratio). Impact strength was measured by the V-notched Izod impact test (based on ASTM D256).

Crazes in a stress-whitened area beneath an impact fracture surface were observed by TEM. Thin sections were cut in a direction perpendicular to or parallel to the fracture surface and observed as indicated in Figure 1. Osmic acid (OsO_4) was used to stain the rubber particles.[14]

It is general knowledge that the higher the gel content is, the higher is the impact toughness which can be obtained under the same rubber content in HIPS. However, while the rubber content and the gel content are almost the same between sample A (D = 0.2 μm) and sample C (D = 4.9 μm), impact toughness is higher for sample C. This suggests that the particle size affects the impact toughness of HIPS even in samples where the rubber content is the same. Hence, the present study was concerned with the toughening mechanism of the bimodal HIPS system, particularly in the system composed of samples A and C.

III. FEM Analysis

Nonlinear stress analysis around rubber particles in HIPS was carried out for uniaxial (Y-axis) tensile loading using FEM. A two-dimensional model was employed under the following conditions: (1) plane strain condition, (2) von Mises' criterion for yielding[15] and (3) rubber particles with a uniform rubbery substance, i.e., neither a "salami" nor "core–shell" structure for simplicity, where

0024-9297/91/2224-5639$02.50/0

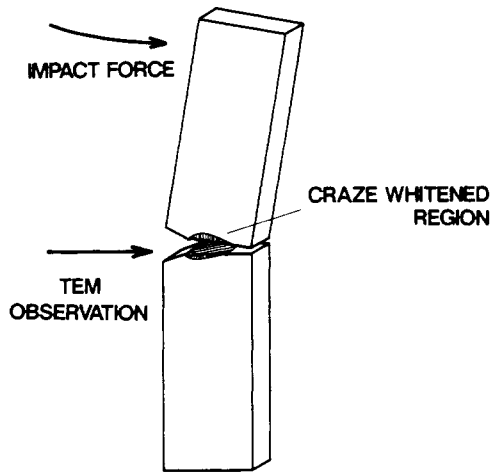

Figure 1. Direction of craze observation in impact fractured specimens by TEM.

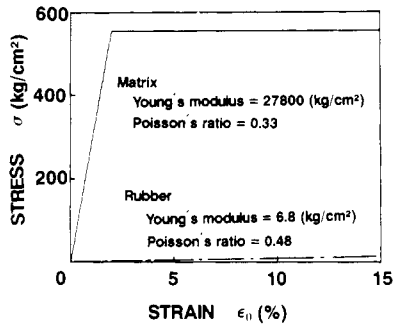

Figure 2. Stress–strain curves used for FEM analysis (for PS matrix and rubber).

Mises' equivalent stress could be expressed as

$$\sigma = 1/2[(\sigma_x - \sigma_y)^2 + (\sigma_y - \sigma_z)^2 + (\sigma_z - \sigma_x)^2 + 6\tau_{xy}^2]^{1/2} \quad (1)$$

On the equatorial plane in our model, tensile directional normal stress was much higher than other stress components. That is, equivalent stress on the equatorial plane is roughly expressed by σ_y.

On the other hand, it is considered that dilatational stress acts as the main factor in crazing. Therefore, we may regard the yielding zone on the equatorial plane as the crazing zone, qualitatively.

In the FEM model, the mesh close to rubber particles was divided into many small partial geometries, because stress concentration seemed to change drastically around the particles in these systems.

Figure 2 shows modeling of the stress–strain curves (S–S curves) of the PS matrix of HIPS and rubbery substances that were employed in the nonlinear FEM analysis.

For the calculation, the FEM program ABAQUS version 4.8 (HK&S, Inc.) together with a CRAY super computer (Model X-MP EA/116SE) owned by Sumitomo Chemical Co. was employed.

IV. Results

(1) S–S Curves. Figure 3 shows the actual S–S curves of HIPS (sample A) and PS having the same molecular weight as HIPS (sample A).

The ultimate (fracture) strain of PS was about 2%; on the other hand, the HIPS sample yielded at a strain of 2% and was fractured at a strain of about 25%. This agreement between the ultimate strain of PS and the yielding strain of HIPS suggests that the latter making crazes were extensively generated in the PS matrix at a strain near 2%. The crazes then grow, and a consecutive

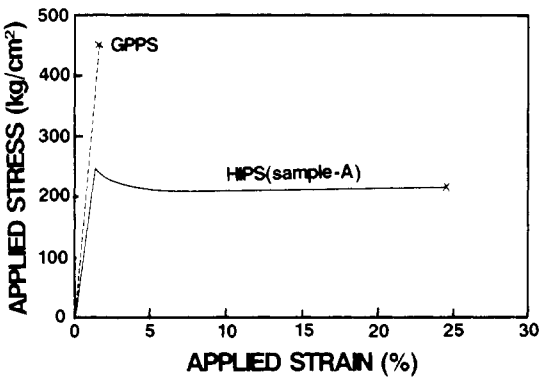

Figure 3. Stress–strain curves of GPPS and HIPS (sample A).

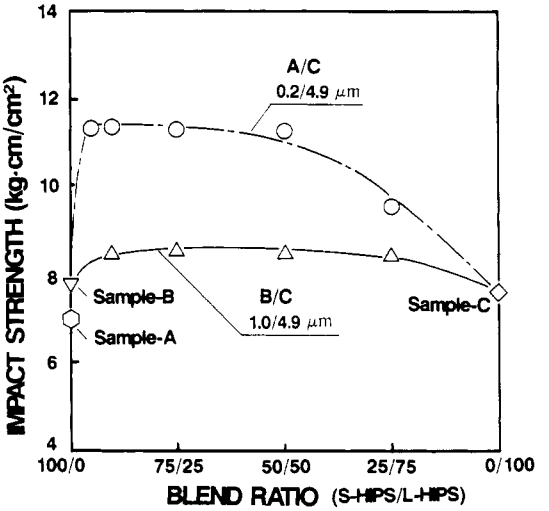

Figure 4. Impact strength vs blend ratio of S-HIPS and L-HIPS. (S-HIPS and L-HIPS are monomodal HIPS with smaller and larger rubber particle sizes in a bimodal HIPS system, respectively. Sample A and sample C are monomodal HIPS of $D = 0.2$ and 4.9 μm, respectively.)

generation of crazes may have followed until the HIPS sample fractured. Therefore, Figure 2 would be acceptable for modeling S–S curves for calculation of nonlinear FEM analysis.

(2) Impact Strength of Bimodal HIPS. Figure 4 shows the relationship between the Izod impact strength and the blend ratios of two different monomodal HIPS for two bimodal systems (sample B/sample C system and sample A/sample C system). Three points are indicated: First, the impact toughness of monomodal HIPS was improved by the blending of two different monomodal HIPS (introducing bimodal HIPS). This effect can be seen in the two bimodal systems in Figure 4. Second, the extent of the improvement effect depends on the particle size ratio in the bimodal system. The greater the difference is between the particle size of the constituent bimodal HIPS, the higher the Izod impact strength is. (The sample A/sample C system has a higher impact toughness than the sample B/sample C system.) Third, as found by Hobbs,[12] the maximum value of the impact strength exists on the S-HIPS-rich side in each bimodal system.

(3) Crazes of Bimodal HIPS. It has been recognized that the impact toughness of HIPS is attributable to the absorption of the applied energy by the generation of crazes,[1-9] and we carefully observed crazes generated in HIPS specimens that applied different impact energy loading. TEM observations were made of whitened regions in front of the initial notch tip in bimodal HIPS samples consisting of samples A and C, and the weight fraction was 9/1.

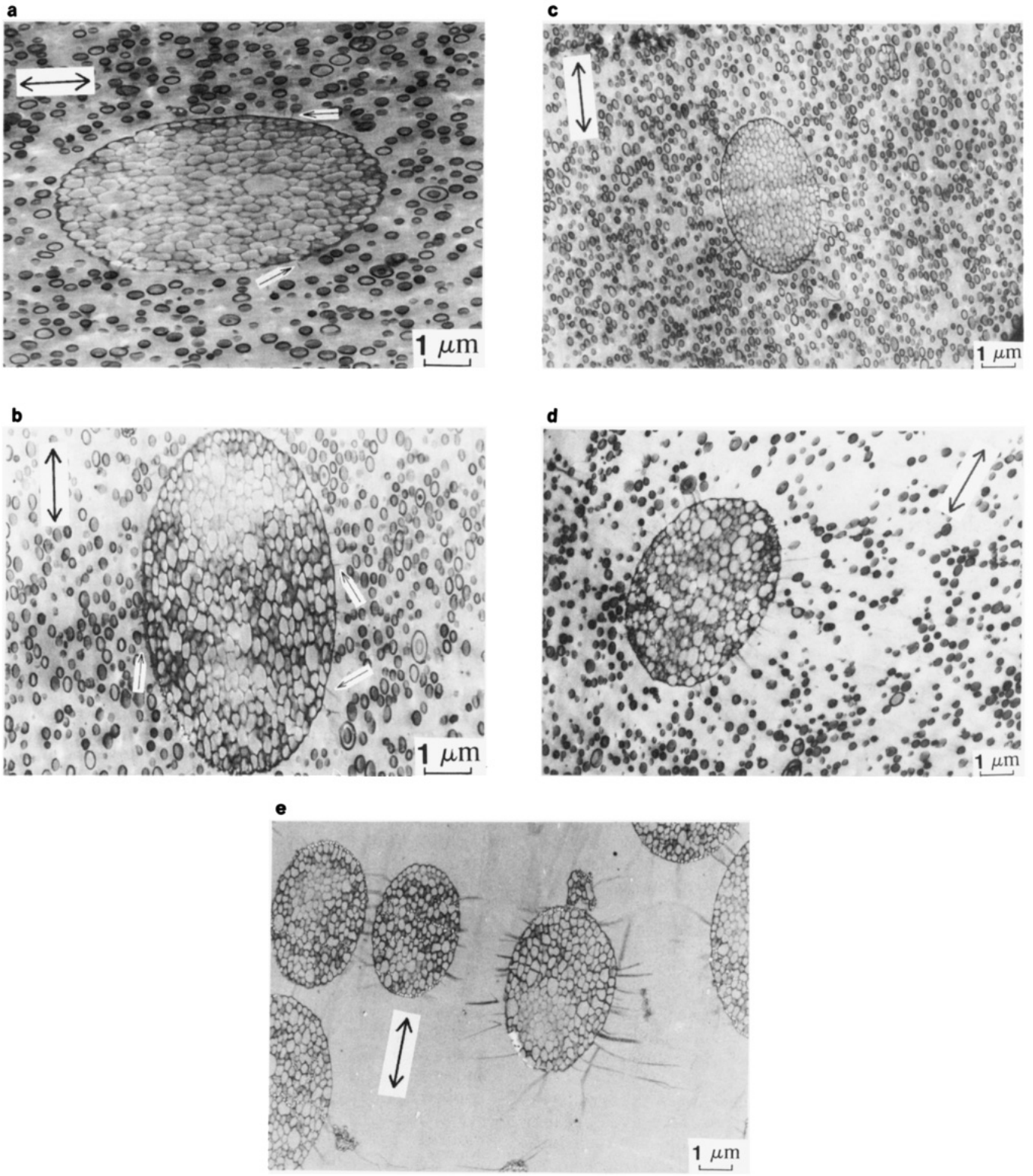

Figure 5. Transmission electron micrographs of crazes. Applied impact energies are (a) 1.2, (b) 3.5, (c) 5.3, and (d) 9.8 kgf·cm (fracture) in b-HIPS and (e) 9.8 kgf·cm in five different specimens of sample C. (The small arrows in a point to minute crazes, and the large arrows in a–e indicate tensile direction. Magnification: (a and b) 14 000, (c–e) 9600.)

Figure 5 shows typical examples of these observations. Impact energies applied for each specimen were (a) 1.2, (b) 3.5, (c) 5.3, and (d) 9.8 kgf·cm (corresponding to fracture) in bimodal HIPS and (e) 9.8 kgf·cm in monomodal HIPS of sample C. As indicated in parts a and b of Figure 5 by arrows, the minute crazes are generated from the large particle surface at the initial stage of craze growth. This is the first step of crazing in bimodal HIPS with a lower applied impact loading. It should be noted that few crazes were observed as initiating from small rubber particles. With greater impact loading, the number of crazes generated from large rubber particles was not much increased, but the crazes became longer (Figure 5c). They originated mainly from the surface of large rubber particles, and their generation sites ranged widely, not being limited around the equatorial plane, due to deformation of the large particles by applied impact loading. In this stage, crazes initiated from the large particles extended bridge-like to neighboring small rubber particles parallel to the equatorial plane. It was not clear, however, whether there

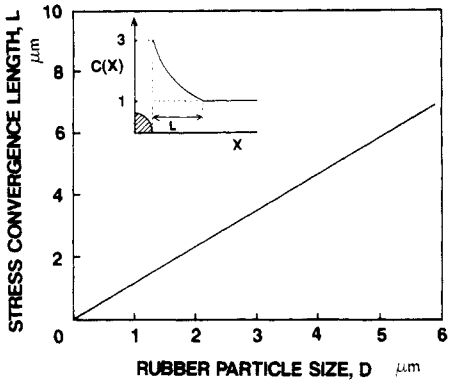

Figure 6. Stress convergence length vs rubber particle diameter. ($C(X)$ is the stress concentration factor and is a function of the distance from the equator of the rubber particle, X.)

were crazes initiated from small particles just ahead of the growing craze tip. Finally, each of the crazes generated from a large particle grew extensively until the length reached 2 or 3 times the equatorial axis of the particle (Figure 5d). Also in this stage, few crazes were observed to initiate from small rubber particles. It is considered that this procedure (parts a–d of Figure 5) represents the aspect of craze growth during the actual Izod impact. Figure 5e shows crazes generated from a rubber particle in monomodal HIPS (sample C in Table I) with large rubber particles ($D_p = 4.9\ \mu m$) corresponding to fracture initiation. Crazes were generated from the periphery of rubber particles perpendicular to tensile loading. A comparison of crazing behavior between bimodal HIPS (Figure 5d) and monomodal HIPS (Figure 5e) after fracture revealed that while the number of crazes was almost the same, the length was much longer (more extensive) in bimodal HIPS than in monomodal HIPS. It is therefore considered that the improved impact of bimodal HIPS is due to the unique growth of long crazes generated at the periphery of the large rubber particles and not to the increase in the number of generated crazes.

(4) Analytical Results of FEM. To investigate this mechanism further, we carried out a stress analysis around rubber particles in bimodal HIPS.

The normal stress concentration factor ($C(X)$) at the equator of a spherical flaw is about 2 by three-dimensional analysis and about 3 by two-dimensional analysis.[16] Nonetheless, semiquantitatively, it is possible to analyze the stress distribution around a spherical flaw by a two-dimensional analysis, which is computationally less complex, and we did so to investigate the crazing mechanism in this study.

Figure 6 shows the relationship between stress convergence length L and rubber particle size D (where L means the distance from the equator of the rubber to the point where the stress concentration factor ($C(X)$) converges with 1). The linear relationship between the stress convergence length and the rubber particle size is apparent.

The distribution of the stress concentration factor around bimodal rubber particles under uniaxial tensile loading is shown in Figure 7, where the loading direction is perpendicular to the equatorial plane and the normal stress for the tensile direction is calculated. Geometries of these models, that is, the rubber particle size and the distance between the particles, were estimated from transmission electron micrographs corresponding to each model in Figure 7. Only the rubber particles existing on the equatorial plane were considered for simplicity in calculation. In Figure 7a, strong stress concentrations which we defined as "bimodal interaction", are exerted at

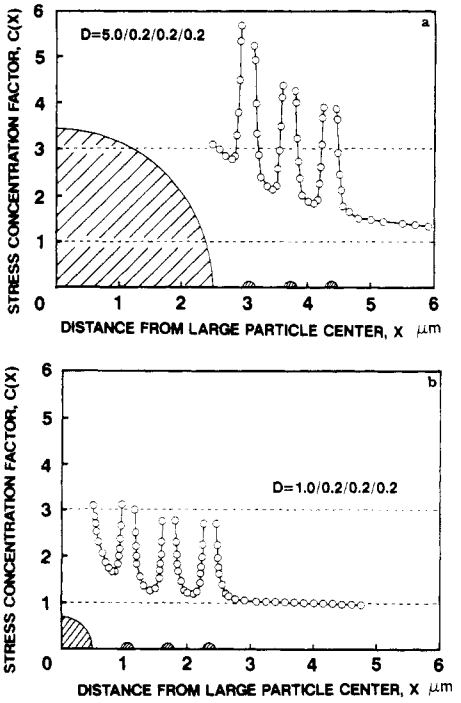

Figure 7. Distributions of the stress concentration factor of bimodal HIPS. The rubber particle diameter (D, μm) ratios are (a) 5/0.2/0.2/0.2 and (b) 1.0/0.2/0.2/0.2.

the surface of the small rubber particles that are located near a large particle. These strong stress concentrations decrease with increasing the distance from the surface of the large particle.

Parts a and b of Figure 7 imply the following: (1) the stress concentration factors of the large rubber particle (5 μm in a and 1 μm in b) are almost the same value (nearly 3); (2) the stress concentration factor at the surface of the small rubber particle located near a large particle of the bimodal system formed with 5.0 and 0.2 μm (corresponding to Figure 7a) is much greater than that of the bimodal system formed with 1.0 and 0.2 μm (corresponding to Figure 7b); (3) as to the length from the equatorial surface of the large particle, at which the stress concentration factors exceed 3, the bimodal system formed with 5.0 and 0.2 μm has a much longer length than the bimodal system formed with 1.0 and 0.2 μm.

To evaluate the growth of the yielding zone, which corresponds to the crazing zone, we carried out nonlinear stress analysis around rubber particles in bimodal HIPS where Mises' equivalent stress was calculated. Figure 8 shows the yielding process varying with an increase of applied strain (ϵ_0) around these particles, where the model geometry is the same as that of Figure 7a; yielding is indicated by cross-hatched areas. In this figure, we focus on the extension of crazes parallel to the equatorial plane of a large particle as seen in Figure 5. Figure 8 shows that crazes in bimodal HIPS grow in the following manner: in a, minute crazes are generated from the surfaces of a large rubber particle and small particle A; in b, the crazes connect with each other, and other crazes generated from small particle B develop. With an increase in the applied strain (c and d), they grow in a manner similar to that above.

V. Discussion

As stated, long crazes may be introduced by bimodal HIPS. The initiation and extension mechanisms of these crazes are discussed below.

(1) Craze Initiation Mechanism. It is considered from Figure 7a (based on linear FEM analysis) that crazes are

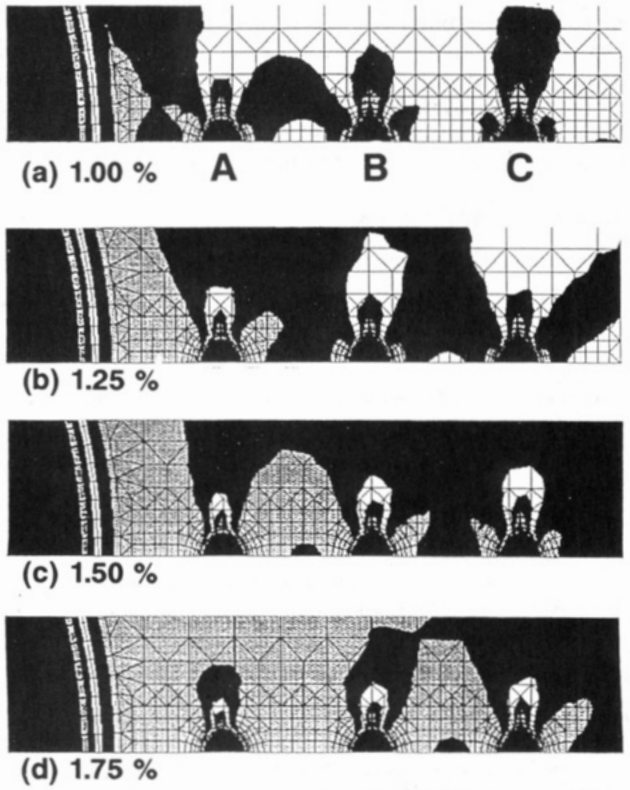

Figure 8. Steps in the expansion of the yielding zone with an increase in applied strain ϵ_0. (The geometry of this model is the same as that of Figure 7a.)

generated from both large and small rubber particles. Figure 8a (based on nonlinear FEM analysis) suggests that craze initiation occurred at both the large particle and small particle (particle A) closest to the large particle. So, it can be considered that craze initiation occurs at the peripheries of both a large rubber particle and a small particle neighboring to the large particle. On the other hand, Kramer and Bucknall suggested that rubber particles smaller than 1 μm rarely initiate crazes.[8,9] As shown in parts a–d of Figure 5, crazes initiated from submicron rubber particles were not observed in these micrographs.

However, we confirmed that submicron rubber particles (D = 0.2 μm) can initiate crazes in an impact fractured specimen of sample A (see the Appendix). That is, rubber particles 0.2 μm in diameter can initiate crazes in bimodal HIPS.

It is therefore believed that craze initiation occurs primarily at a large rubber particle and that minute crazes can be initiated supplementarily from small particles (0.2 μm).

(2) Craze Extension Mechanism. Parts a–d of Figure 8 imply that the yielding zone generated from a large particle extends like a bridge to neighboring small rubber particles. This feature of craze extension is consistent with the results of TEM observation (Figure 5a–d).

The craze extension mechanism described above is illustrated schematically in Figure 9; however, this model is different from that proposed by Hobbs[12] and that of Wrotecki and de Charentenay.[13] The latter researchers analyzed stress distribution around bimodal rubber particles using FEM analysis and suggested that crazes may initiate from small rubber particles in the vicinity of large particles and that they were stopped by the large particles. Our model (Figure 9), however, indicates that the large particle acted as craze initiator but not as craze terminator.

With regard to the mechanism governing the improved impact of bimodal HIPS, the breadth of the stress field

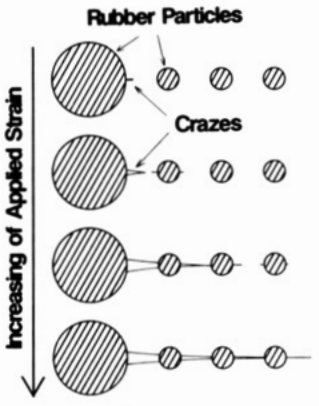

Figure 9. Schematic model of the craze extension with an increase of applied strain.

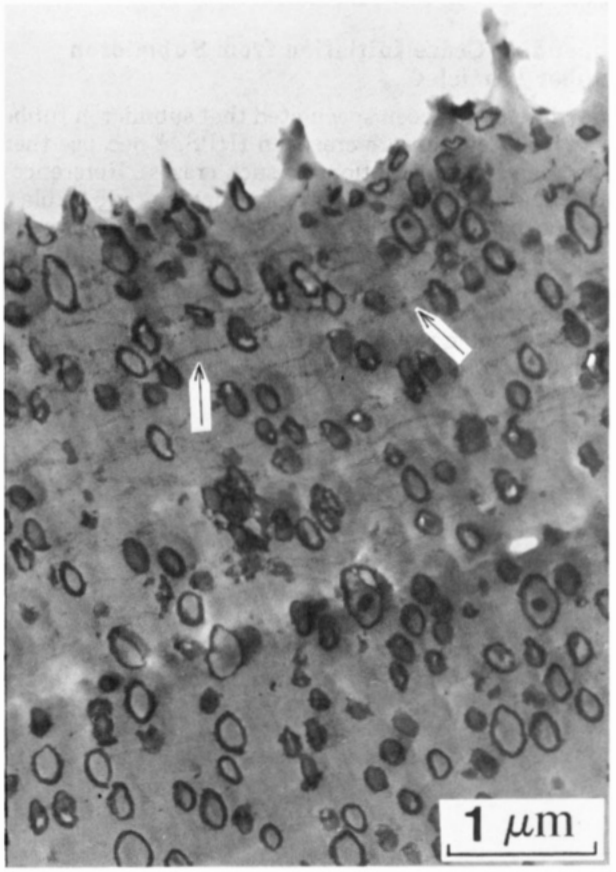

Figure 10. Crazes from rubber particles 0.2 μm in diameter. Crazes were observed in Izod impact fractured specimens of sample A.

of large rubber particles is one of the most important points. Stress convergence length (which corresponds to the effective stress field for craze generation) of a rubber particle is proportional to particle size as shown in Figure 6. The stress convergence length of a small (D = 0.2 μm) and a large particle (D = 4.9 μm) in our bimodal system is in the ratio 1:25. Thus, the effective stress field of the large rubber particle is more extensive than that of the small one.

The second point is the shorter distance between rubber particles. Under a constant rubber content, the smaller the particle is, the shorter is the distance between particles. Judging from the equation derived by Wu,[17] the ligament thickness, τ (distance between two rubber particle surfaces), in monomodal HIPS is proportional to the rubber

particle size

$$\tau = D[(\pi/6\phi_r)^{1/3} - 1] \quad (2)$$

where D is the average rubber particle size and ϕ_r is the rubber volume fraction; thus, the ligament thickness of sample A to that of sample C is in the ratio 1:25. Hence, a large number of small particles in bimodal HIPS results in a thin ligament thickness.

These two effects can be achieved by bimodal distribution of the rubber particle size in HIPS. They will cause longer crazes, and, consequently, a higher impact strength can be obtained in bimodal HIPS compared with that in monomodal HIPS.

Acknowledgment. We thank Mr. Mikio Hirai and Mr. Kazunori Takahashi for their generous support and suggestions with the TEM work.

Appendix: Craze Initiation from Submicron Rubber Particles

To date, it has been speculated that submicron rubber particles rarely initiate crazes in HIPS,[8,9] because there have been few observations of such crazes. Reference 6 in particular reported that the feature is attributable to very localized stress concentration. To investigate this more deeply, TEM observations were made of impact fractured specimens of monomodal HIPS containing rubber particles 0.2 μm in diameter. The micrograph in Figure 10, taken just below the fracture surface ahead of the initial notch tip, shows crazes generated from submicron rubber particles. It is obvious that these grew perpendicular to the applied stress acting on the extended crack tip. This result not only suggests that submicron rubber particles can initiate crazes in spite of the localized stress field but also supports the validity of our proposed model of the craze initiation mechanism.

References and Notes

(1) Bucknall, C. B. *Toughened Plastics*; Applied Science: London, 1977.
(2) Keskkula, H. *Rubber-Toughened Plastics*; American Chemical Society: Washington, DC, 1989; p 289.
(3) Boyer, R. F.; Kesukkula, H. *Encycl. Polym. Sci. Technol.* **1982**, *13*, 392.
(4) Angier, D. J.; Fettes, E. M. *Rubber Chem. Technol.* **1965**, *36*, 1164.
(5) Moore, J. D. *Polymer* **1971**, *12*, 478.
(6) Donald, A. M.; Kramer, E. J. *J. Appl. Polym. Sci.* **1982**, *27*, 3729.
(7) Bucknall, C. B.; Smith, R. R. *Polymer* **1965**, *6*, 437.
(8) Bucknall, C. B. *Polymer Blends*; Paul, D. R.; Newman, S., Eds.; Academic: New York, 1978; Vol. 2, p. 99.
(9) Donald, A. M.; Kramer, E. J. *J. Mater. Sci.* **1982**, *17*, 2351.
(10) BASF. U.S. Patent 4,493,922.
(11) Sumitomo Chemical Co. U.S. Patent Appl. 07/223, 599.
(12) Hobbs, S. Y. *Polym. Eng. Sci.* **1986**, *26*, 74.
(13) Wrotecki, C.; de Charentenay, F. X. *Deform. Yield. Frac. Polym.* **1988**, *7*, 51/1.
(14) Kato, K. *Polym. Lett.* **1966**, *4*, 35.
(15) von Mises, Z. *Angew. Math. Mech.* **1928**, *8*, 161.
(16) Goodier, J. N. *J. Appl. Mech. Trans. ASME* **1933**, *55*, A39.
(17) Wu, S. *Polymer* **1985**, *26*, 1855.

Registry No. PS (homopolymer), 9003-53-6.